



Characterization of proposed waste disposal site of granite quarry pits near Hyderabad using hydro-geophysical and groundwater modeling studies

Ratnakar Dhakate¹ · Nandan Jayaraja Mogali¹ · Durgaprasad Modi¹

Received: 25 June 2020 / Accepted: 29 July 2021 / Published online: 9 August 2021
© The Author(s), under exclusive licence to Springer-Verlag GmbH Germany, part of Springer Nature 2021

Abstract

Safe disposal and storage of dredged sediments from severely polluted urban lakes is a big challenge to deal with. This paper deals with the importance of hydro-geophysical and groundwater modeling applications for characterizing appropriate and environmental safe site for storage and disposal of hazardous dredged sediment from Hussain Sagar Lake bed. One such disposal site is proposed at Gajularamaram village near Quthbullapur Mandal, Greater Hyderabad. The area is having predominantly exposed rocks of Peninsular Gneissic Complex (PGC) along with enclaves of schists and basic dykes. The geological singularities are the major concern for an environmentally protected construction of the landfill. Hydro-geophysical studies, such as Electrical Resistivity Tomography (ERT), water level monitoring and in situ soil infiltration tests carried out in and around the proposed waste disposal granite quarry site. In situ soil infiltration rate varied from 0.09 to 15.36 cm/hr. Besides, groundwater flow and mass transport model was conceptualized for predicting any seepages of leachate from these waste filled quarry pits. The results indicated that the existing abandoned granite quarry pits are suitable for disposal of hazardous lake bed sediment of Hussain Sagar Lake. Furthermore, few remedial measures were suggested for arresting lateral migration of leachate if any through quarry pits.

Keywords Electrical resistivity tomography (ERT) · Infiltration test · Waste disposal site · Greater Hyderabad

Introduction

Now-a-days, the issue of anthropogenic contamination by solid and liquid wastes in the environment is one of the primary concerns for researchers. Rapid urbanization and fast industrial development has resulted in the production of hazardous and non-hazardous solid and liquid residues. Hazardous and non-hazardous dredging material and environmental pollutants are generally dumped inefficiently in waste disposal sites posing serious threat to the groundwater resources, environment and the community health. Hence, it is essential to dispose the hazardous dredged material in a proper and environmentally suitable site. One problem which confronts environmentalist and city planners worldwide is

the issue of efficient management of solid waste (Mirbagheri and Esfeh 2008). Landfills have created various problems such as surface and groundwater contamination (Abushamala et al. 2010; Alslaibi et al. 2011).

Recently, there is a rising alarm all over the world for the treatment and disposal of hazardous and non-hazardous waste generated through anthropogenic sources. The waste generators find it difficult for safe disposal without disturbing environment. As of now, very few appropriate disposal facilities are available in the countries like India. The disposal of hazardous waste needs a proper and secured site suitable typical to waste's properties viz., toxicity, corrosivity, ignitability, reactivity and persistence. Broad range of health hazard risks has been accredited to their contamination. Varieties of options are available for the treatment and safe disposal of hazardous waste in a safe environmental protection conditions (Wentz 1995). However, it reveals that, more options were available for hazardous waste management (HWM) were not being efficiently used by the waste generators and resulting in severe contamination of

✉ Ratnakar Dhakate
dhakate.ratnakar@gmail.com

¹ CSIR-National Geophysical Research Institute, Council of Scientific and Industrial Research Institute, Uppal Road, Hyderabad 500 007, India

groundwater, surface water and land (Kenny 1995; Praful 1996; Sunny 1997; Nair 1999).

It is very difficult to find a suitable site for disposal facility or landfills locations in terms of geological and geotechnically suitable in metropolitans cities (Allen et al. 1997; Bagchi 1994; EPA 1995, 1996, 1997, 1999a, b; DELG 1998, 1999; Hillary and Samuel 1993; Langer 1995; Mather 1995; Georgaki et al. 2006). Details on the contents of a landfill may be difficult to acquire but are essential for evaluating the level of risk associated with leaking pollutants (Beres and Haeni 1991; Davis and Anan 1989; Green et al. 1999; Heitfeld and Heitfeld 1997; Lanz et al. 1994; Orlando and Marchesi 2001; Soupios et al. 2005a; b; c; Saltas et al. 2005). Electrical method (resistivity technique) found to be very suitable for selection of disposal site or landfills due to the sub-surface characterization and conductive nature of most of the contaminants. These techniques have been used successfully by many researchers for characterization of safe and environmentally protected disposal sites and landfills (Atekwana et al. 2000; Sauck et al. 1998; Sauck 2000; Stanton and Schrader 2001; Karlik and Kaya 2001; Bernstone et al. 2000; Aristodemou and Thomas-Betts 2000; Dawson et al. 2002). To evaluate the capabilities and limitations of geophysical methods in providing accurate information on typical waste dump sites and their host sediments, we have conducted surveys over and around abandoned stone granite quarry pits in Gajularamaram, Greater Hyderabad.

Integrated geophysical, hydrogeological, groundwater flow and mass transport modeling study provides an important tool in the evaluation and characterization of contaminants (Jorge et al. 2004). Appropriate waste disposal facility should be properly characterized by carrying out hydrogeological and geophysical investigations in a safe environmental construction of disposal facility (Li-Wen et al. 2006). Environmentalists, health workers and city planners are facing a problem for efficient management and disposal of toxic and non-toxic waste generated in metropolitan cities in India. An integrated investigation was carried out to evaluate and identify the safe and suitable site for disposal of waste with no consequence impact on the environment and surrounding habitations.

The Hussain Sagar Lake is situated in the heart of Hyderabad city and receives toxic substances from four major streams draining from a catchment area of 275 km². Discharges from these major streams contain urban, municipal and industrial effluents containing toxic and non-toxic elements (Srikanth et al. 1993; Jain et al. 2010). The effluents contain heavy metals and get adsorbed onto the sediments and settle down to the bottom of the lake (Jain et al. 2010). Authorities of Hyderabad Urban Development Agency (HUDA) plan for the safe disposal of these toxic sediments in the abandoned granite quarry pits situated at Gajularamaram village in Quthubullapur Mandal

in the out-skirts of Hyderabad city. To assess the present conditions of these quarry pits, detailed hydrological and geophysical investigations were carried out in and around these quarry pits to map the near surface features in hard rock terrain and their suitability for further safe dumping of hazardous waste from Hussain Sagar Lake bed sediments. Further groundwater flow and mass transport modeling was carried out to examine the seepages of contaminants from these quarry pits.

Study area

The proposed disposal site area lies between latitudes 17° 30' 0"–17° 32' 30" N and longitudes 78° 22' 30"–78° 27' 30" E is located at Gajularamaram Village, Quthubullapur Mandal, Ranga Reddy District, Telangana State, India. The area occupies the Survey of India topo sheet No. 56 K/6/SE with a scale of 1:25,000 cm. Lal Sahebguda and Kaiser Nagar village habitations are on the upstream side and Mettakadigudem habitation is situated on the eastern part of proposed site (Fig. 1). The watershed covers an area of about 19.7 km² having dimensions of 4.2 × 4.7 km is in the downstream of the pit. The drainage pattern is sub-dentric. No significant lineament is passing through the proposed quarry pits. The pits were excavated up to a depth of 12–15 m (bgl) having perimeter 567 m and 347 m for Pit-1 and Pit-2, respectively.

Hussain Sagar lake bed sediments quality

Hussain Sagar, the scenic lake situated between the twin cities of Hyderabad and Secunderabad, is an ecological and cultural landmark for the twin cities. It was constructed during the year 1562 mainly to store drinking water brought from the Musi River, a tributary of Krishna River, one of the major rivers of South India. The lake represents one of the thousands of impoundments on Deccan plateau in peninsular India, developed for storage of surface water runoff generated during monsoon. It lies 510 m (amsl) and covers a catchment watershed area of 275 km² and divided into four sub-basins viz., Kukatpally, Dullapally, Bowanpally and Yusufguda. The highest elevation in the catchment is at 642 m (amsl) at north and lowest elevation of 500 m (amsl) near tank bund. The lake was feeded by four major in-lets (nallas) viz. Kukatpally, Picket, Banjara and Balkapur. Out of the four in-lets, Kukatpally in-lets passes through two major industrial areas viz. Kukatpally and Balanagar and it is the main feeding channel to the lake. The lake receives heavy metals through urban runoff as well as municipal sewage and industrial effluents. Heavy metals entering into the lake get adsorbed onto the suspended sediments and settle down in the bottom sediments. The fractionation of metal ions on the bed sediments of Hussain Sagar Lake was

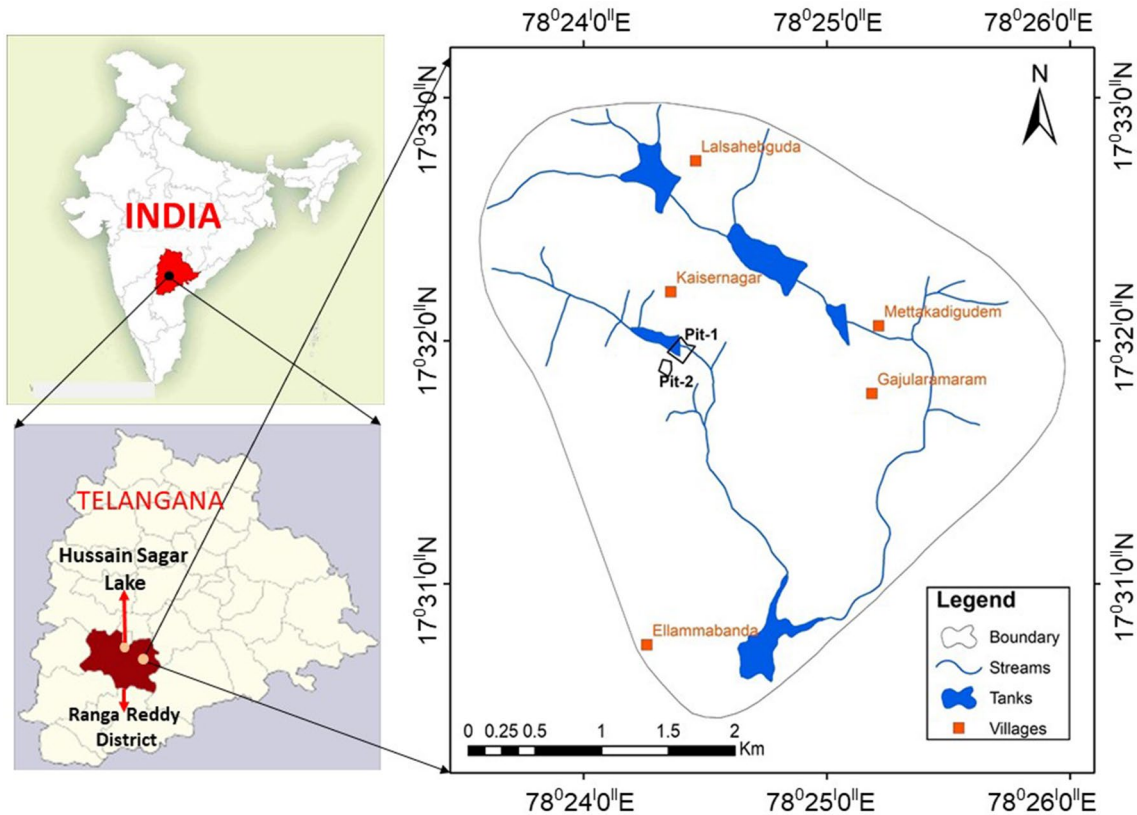


Fig. 1 Location map of study area, Gajularamaram, Greater Hyderabad

studies by Jain et al. (2010) and others were also reported the heavy metals in groundwater surrounding the lake (Srikanth et al. 1993). The heavy metals present in lake sediments are shown in Fig. 2 (Jain et al. 2010).

Geology and hydrogeology

The area is having predominantly exposed rocks of Peninsular Gneissic Complex (PGC) along with enclaves of schists and basic dykes. No significant lineament is passing through the proposed dump site. The schists include mainly amphibolites, hornblende, biotite schist, occasional quartzite, ferruginous quartzite, pyroxene granulite, talc schist, quartz and sericite schist. Granite is widely distributed throughout the area, it is grey to pink in color, medium to coarse-grained in size and massive porphyritic or non-porphyritic in composition (Fig. 3) (Bhukosh GSI <http://bhukosh.gsi.gov.in/Bhukosh/Public>). It occupies higher topographic levels forming denudation hills, dome-shaped mounds and boulder outcrops. The watershed is in the granite and granite gneiss rocks and area is mostly covered with pediment inselberg complex (PIC), Pediplain shallow (PPS) and Valley Fill Shallow (VFS) geomorphologic features. A second-order stream originates and it is traverses up to Ellammabanda

tank in the downstream before leaving the study area. Another stream originating from Lal Sahebuda passes close to the Gajularamaram village and Mettakadigudem joins the Ellammabanda tank in the downstream.

Materials and methods

Hydrogeological investigation

Groundwater monitoring was carried out on selected 34 observation wells during July 2013 with in situ TDS measurements (Table 1 and Fig. 4). Besides, in situ soil infiltration measurements on the ground surface as well as in the quarry pit bottom were made using a double ring infiltrometer (Fig. 5). The results of in situ infiltration rate along with ERT's Nos. (Table 2).

Electrical resistivity tomography (ERT)

ERT provide opportunity for imaging the sub-surface resistivity distribution and to detect and differentiate the various features in the sub-surface formation. Electrical Resistivity

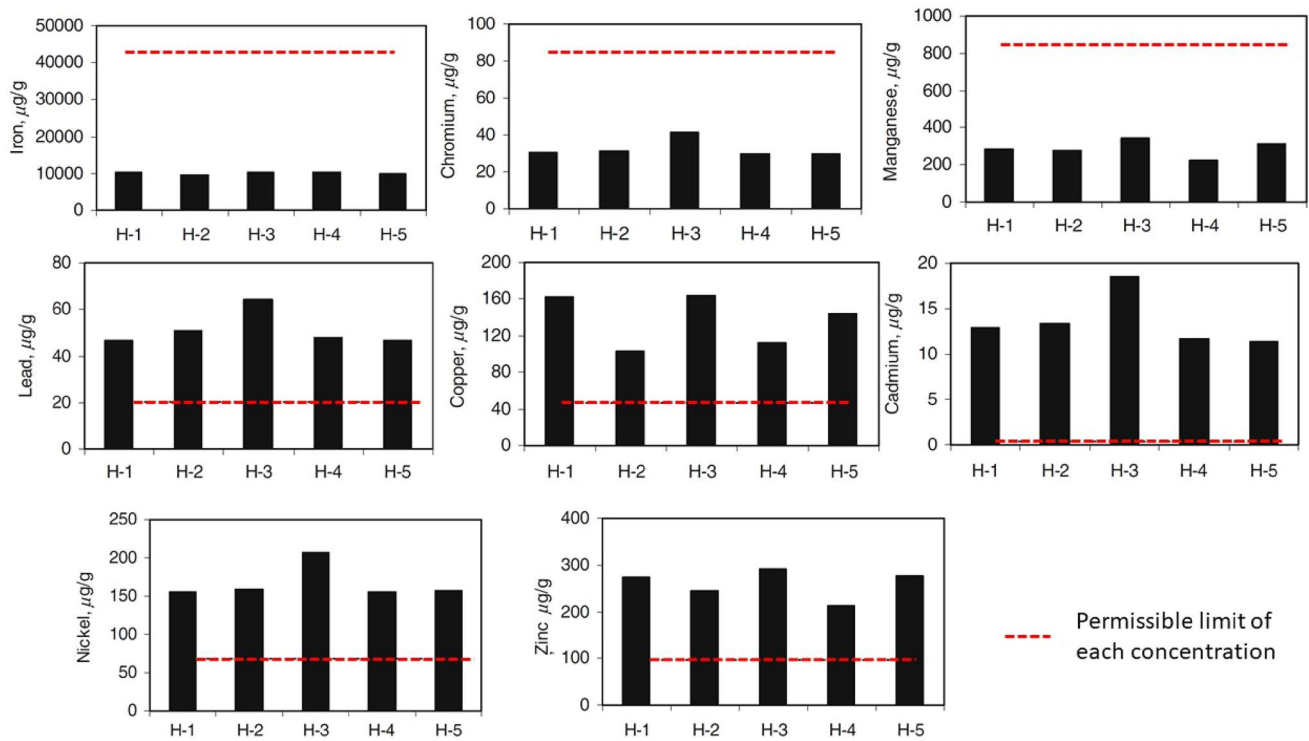


Fig. 2 Heavy metals contamination (µg/g) in Hussain Sagar lake bed sediments (after Jain et al. 2010)

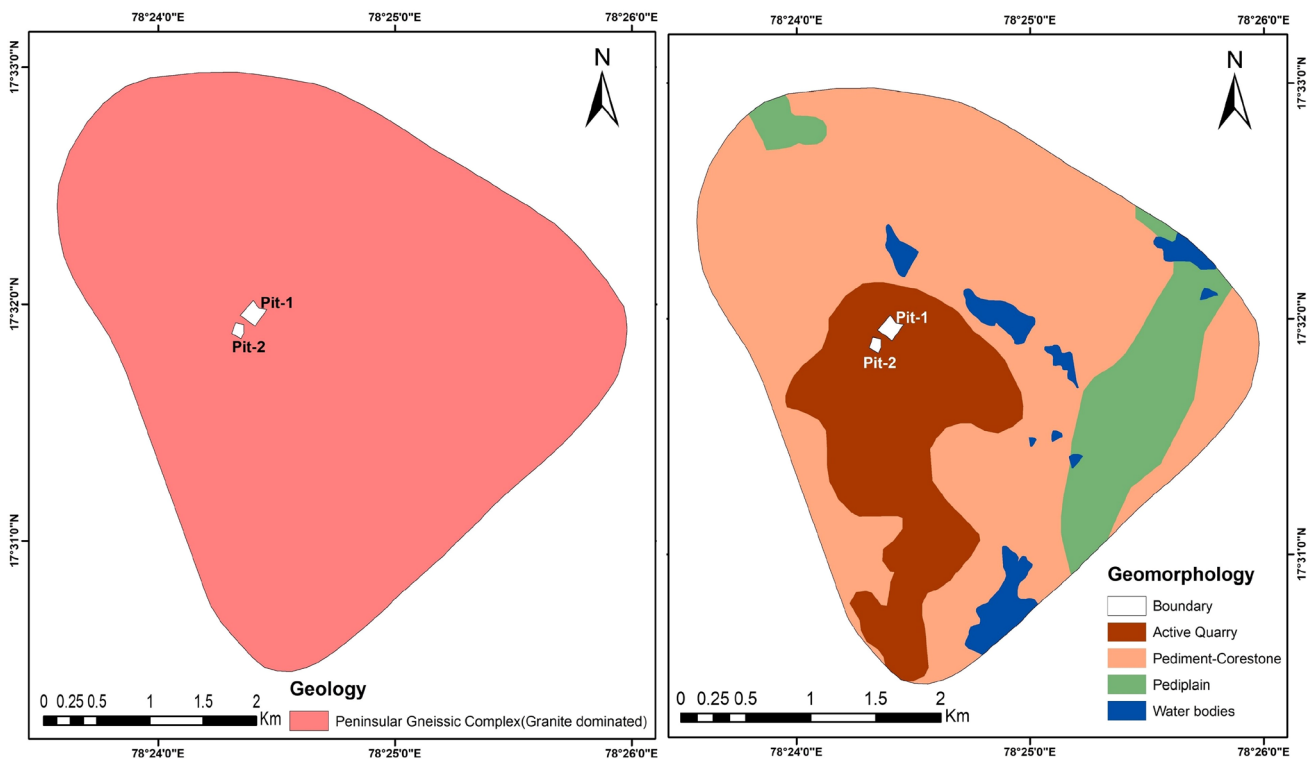


Fig. 3 Geology and geomorphology map of the study area (source: Bhukosh GSI)

Table 1 Observation wells for groundwater monitoring in the watershed

Well no	RL m (amsl)	Depth to water level m (bgl)	Groundwater level m (amsl)	TDS (mg/l)
G1	588	21.91	566.09	570
G2	589	25.56	563.44	420
G3	610	26.71	583.29	1490
G4	612	27.49	585.29	1350
G5	607	26.6	580.40	1580
G6	588	26.11	561.89	720
G7	588	26.32	561.68	850
G8	589	26.88	562.27	1100
G9	593	26.73	566.12	840
G10	591	26.86	564.14	750
G11	595	22.92	572.08	510
G12	587	20.09	566.91	500
G13	586	20.87	565.13	410
G14	589	21.38	567.62	440
G15	585	20.89	564.11	510
G16	590	22.78	567.22	530
G17	595	23.53	571.47	440
G18	596	23.68	572.32	360
G19	593	23.22	569.78	540
G20	600	27.91	573.99	710
G21	576	18.9	557.10	270
G22	574	18.49	555.51	420
G23	573	18.28	554.72	250
G24 (DW)	572	18.11	553.89	280
G25	577	19.72	558.00	370
G26	574	19.54	555.03	330
G27	578	19.06	559.11	230
G28	579	19.04	559.96	260
G29	581	23.66	557.34	570
G30	582	24.52	557.48	560
G31	580	19.53	560.47	390
G32	583	19.02	563.98	420
G33	584	19.88	564.12	490
G34	585	19.41	565.59	540

RL reduced level, bgl below ground level, amsl above mean sea level

Tomography (ERT) is the latest technology used to determine the sub-surface resistivity laterally and vertically simultaneously. ERT system produces a pseudo-section image showing the distribution pattern of electrical resistivity of the sub-surface formations. This technique employs a multi-electrode arrangement. In this technique, all the electrodes were spread along a straight line and are connected with connectors to a cable. The cable is connected to an ERT imaging system. The system injects current between a pair of electrodes and measures the resultant voltage difference

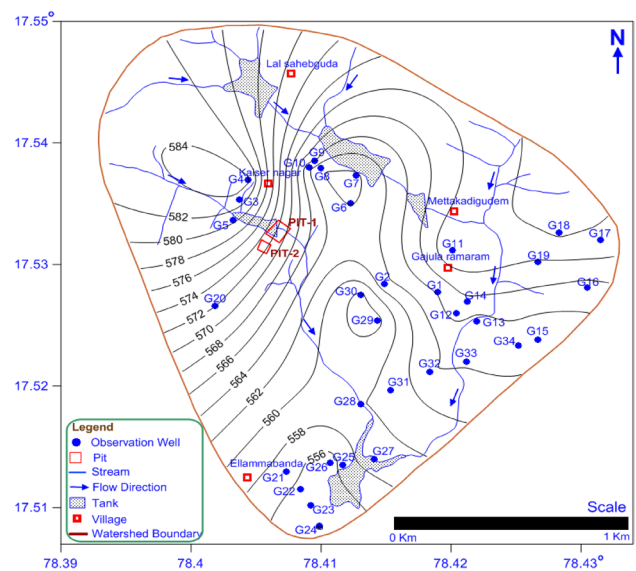


Fig. 4 Groundwater level in m (amsl) and flow direction in the study watershed

between remaining electrode pairs according to a pre-defined measurement protocol. The electrodes are connected to the data acquisition system by co-axial cable which assists in reducing the effect of extraneous environmental noise and interference. The data must be collected quickly and accurately to track small changes of resistivity/conductivity in real-time allowing the image reconstruction algorithm to provide an accurate measurement of the true resistivity/conductivity distribution. In four electrode arrangement (for e.g. electrodes 1, 2, 3 and 4) current is applied through two electrodes (e.g. electrodes 1 and 4). The voltage is measured from the remaining pairs of electrodes (e.g. electrodes 2 and 3). With constant electrode spacing, the procedure is repeated along a profile by skipping first electrode in the previous measurement and adding successive electrode to the four electrode arrangement until the profile is completed. Similar such procedure is repeated on the same profile with increased electrode spacing to get measurements from the deeper depths. In the ERT system, the reconstructed image would contain information on the cross-section distribution of the electrical resistivity/conductivity of the medium within the measured plane.

Sub-surface conditions in the watershed covering the proposed waste disposal site of granite quarry pits was assessed by ERT imaging system deployed at 22 locations using Wenner-Schlumberger Configuration to determine the sub-surface characteristics (Fig. 5). The processing and interpretation of geoelectrical data were performed using the RES2DINV algorithm, which generates a two-dimensional (2D) resistivity depth model of the sub-surface resistivity distribution. The 2D resistivity model is obtained using the

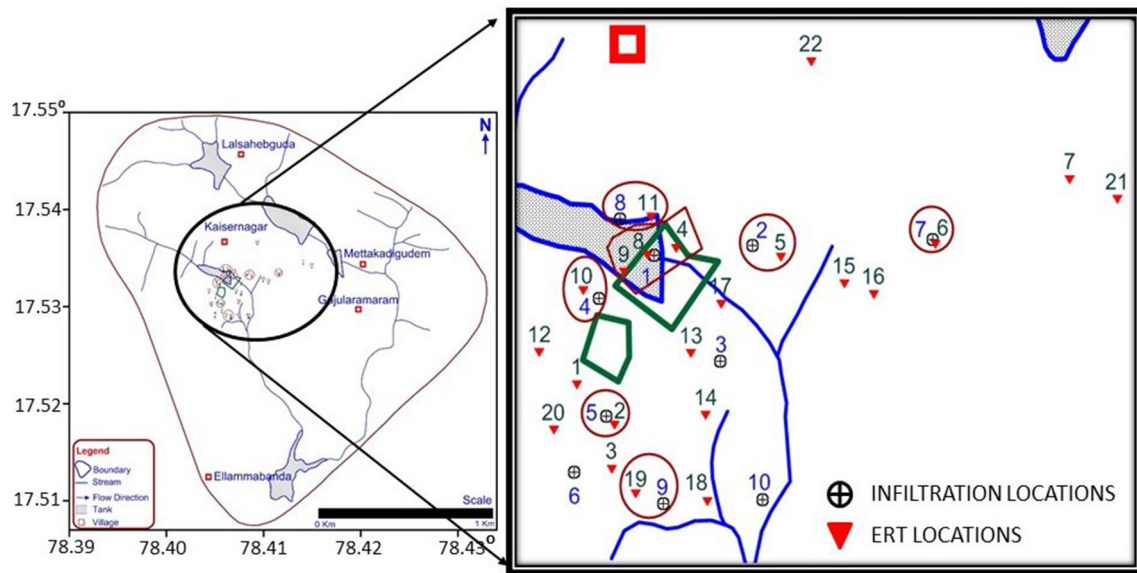


Fig. 5 Electrical resistivity tomography (ERT) and in situ infiltration tests locations carried out in the study watershed

Table 2 In-situ infiltration rate (cm/hr) in the watershed covering the granite quarry pits, Gajularamaram, Quthubullapur Mandal, R.R. District

S. no	Location	Infiltration test no	Rate of infiltration (cm/hr)	Correlated ERT's	Resistivity values ranged (Ω m)	Interpreted formation
1	Inside Pit-1	1	0.42	ERT 8 ERT 4 ERT 9	828–92,019 558–398,651 4652–336,903	Hard to very hard rock Hard to very hard rock Hard to very hard rock
2	North-eastern side far away from Pit-1	2	0.25	ERT 5	15.3–49.2 158 509–54,669	Saturated weathered Semi-weathered Hard to very hard rock
3	South-eastern side of Pit-1	3	0.51	–	–	–
4	In-between Pit-1 and Pit-2	4	0.09	ERT 10	27.8–73.9 197 523- 26,220	Saturated weathered Semi-weathered Hard to very hard rock
5	Southern side of Pit-2	5	10.2	ERT 2	16.9–50.9 153–461 1388–37,847	Saturated weathered Semi-weathered/fractured Hard to very hard rock
6	Sothern side far away from Pit-2	6	7.6	–	–	–
7	Eastern side far away from Pit-1	7	0.51	ERT 6	6.03–16.4 44.7–332 903–6691	Saturated weathered Weathered/Semi-weathered Hard to very hard rock
8	North side of Pit-1 near tank	8	1.53	ERT 11	11.2–21.7 41.8–80.6 156–300 579–1117	Saturated weathered Weathered Semi-weathered/fractured Hard rock
9	Southern side far away from Pit-1 and Pit-2	9	10.2	ERT 19	23.9–68 194 552–36,310	Saturated weathered Semi-weathered Hard to very hard rock
10	South-eastern side far away from Pit-1 and Pit-2	10	15.4	–	–	–

standard Gauss–Newton method to the measured data (Loke and Barker 1996). The inversion procedure iterates to fit with a low RMS error and thus one assumes that the interpreted resistivity of formations depict a realistic image of the sub-surface resistivity.

Groundwater flow modeling

To understand the movement of pollutant and seepages from the quarry pits in to the surrounding groundwater regime in the watershed, an attempt has been made to construct a mathematical model using Visual MODFLOW software for Windows version 2.61 (Guiger and Franz 1996). Essentially, mathematical model of a system implies obtaining solutions to one or more partial differential equations describing groundwater regime (Konikow and Grove 1977). In the present case, it was assumed that the groundwater system is a two-dimensional one, wherein the Dupuit–Forchheimer condition is valid. The partial differential equation describing two-dimensional groundwater flow may be written for a homogeneous aquifer system as

$$\frac{\partial}{\partial y} \left(T_x \frac{\partial h}{\partial y} \right) + \frac{\partial}{\partial x} \left(T_y \frac{\partial h}{\partial x} \right) = S \frac{\partial h}{\partial t} \pm W, \tag{1}$$

where T_x, T_y = transmissivity values along x and y directions, h = hydraulic head, S = storativity, W = groundwater volume flux per unit area (+ve for outflow and –ve for inflow), x and y = Cartesian co-ordinates.

Mass transport modeling

An equation describing the transport and dispersion of a dissolved chemical in flowing groundwater may be derived from the principle of conservation of mass by considering all fluxes. A generalized form of the solute transport equation, in which terms are incorporated to represent chemical reactions and solute concentration both in the pore fluid and on the solid surface, as:

$$\frac{\partial(\epsilon C)}{\partial t} = \frac{\partial}{\partial x_i} \left(\epsilon D_{ij} \frac{\partial C}{\partial x_j} \right) - \frac{\partial}{\partial x_i} (\epsilon C V_i) - C' W^* + CHEM, \tag{2}$$

where CHEM equals one or more of the following:

$-\rho_b \frac{\partial \bar{C}}{\partial t}$ for linear equilibrium controlled sorption or ion-exchange reactions $\sum_{k=1} R_k$ for chemical rate-controlled reactions, and (or) $-\lambda \left(\epsilon C + \rho_b \bar{C} \right)$ for decay and where D_{ij} is coefficient of hydrodynamic dispersion (a second-order tensor) $L^2 T^{-1}$, C' is the concentration of the solute in the source or sink fluid, C is the concentration of the species adsorbed on the solid (mass of solute/mass of solid), ρ_b is the bulk

density of the sediment ML^{-3} , R_k is the rate of production of the solute in reaction k , $ML^{-3} T^{-1}$, and λ is the decay constant T^{-1} .

The coefficient of hydrodynamic dispersion is defined as the sum of mechanical dispersion and molecular diffusion (Bear 1979). The mechanical dispersion is a function of both the intrinsic properties of the porous medium (such as heterogeneities in hydraulic conductivity and porosity) and of the fluid flow. These relations are commonly expressed as

$$D_{ij} = \alpha_{ijmn} \frac{V_m V_n}{|V|} + D_m \quad i, j, m, n = 1, 2, 3... \tag{3}$$

where α_{ijmn} is the dispersivity of the porous medium (a fourth-order tensor), L ; V_m and V_n are the components of the flow velocity of the fluid in the m and n directions, respectively, LT^{-1} , D_m is the effective coefficient of molecular diffusion, $L^2 T^{-1}$; and $|V| = \text{sq root } V_x^2 + V_y^2 + V_z^2$ (Bear 1979; Domenico and Schwartz 1990).

Results and discussion

Groundwater occurs under the water table condition in granitic formations at 20–25 m (bgl) and semi-confined to confined condition at depth. The depth to groundwater is varying from 18.11 m (bgl) in the valley part in the downstream of Ellammabanda tank to 27.49 m (bgl) near Kaiser Nagar. Maximum depth to groundwater was noticed around the proposed waste disposal site of granite quarry pits (Fig. 4). The yield of bore wells was poor < 15 LPS in Kaiser Nagar and Lal Sahebguda villages and these habitations depend mostly on the stored surface water in the excavated quarries nearby. The absolute elevation of groundwater is varying from highest elevation of 585 m (amsl) near Kaiser Nagar to 554 m (amsl) in the bore well near the outflow region of Ellammabanda tank during July 2013 (pre-monsoon) (Fig. 4). The groundwater flow direction was ascertained from the groundwater level contours indicate that it flows from Kaiser Nagar towards Gajularamaram village maintaining steep hydraulic gradients from north-west to south-east. The groundwater levels around the Ellammabanda tank maintains slightly mild slope.

A total of 10 in situ soil infiltration tests were conducted in the study area to observe the infiltration rate of the soil (Fig. 5). The results of infiltration test are shown in Table 2. Geophysical investigations using ERT have been carried out at 22 locations in the study area as shown (Fig. 5). The Wenner-Schlumberger array with 1 m, 2 m and 5 m electrode spacing was used to collect resistivity data as the array can effectively represent signal/noise ratio as well as effective resolution, which is an important parameter while representing resistivity. The geoelectrical profiles revealed

resistivity values that varied lateral and vertical aspect with depth, could be differentiated with the resistivity signatures obtained from ERT images. The ERT images which are carried out in the close vicinity of the infiltration test sites were correlated and discussed below.

Infiltration test No.1 was carried out inside the Pit-1 and its rate of infiltration was 0.42 cm/hr. Near this test site, ERT profile No. 8 was carried out using 48 electrodes with 2 m electrode separation. The ERT image shows a hard to very hard rock formation with resistivity $> 828\text{--}92,019 \Omega\text{m}$ up to an entire depth profile (Fig. 6). Similarly, close to infiltration test No. 1, another ERT's Nos. 4 and 9 using 24 electrodes with 1 m and 5 m separation were also carried out inside and outside the Pit-1 showing similar ranges of resistivity. ERT

No. 4 exhibit a resistivity $> 558 \Omega\text{m}$ to very high and ERT No. 9 exhibit a resistivity $> 4652 \Omega\text{m}$ to very high indicating a hard to very hard rock formation (Fig. 6). Infiltration test No. 2 was carried out in north-eastern side far away from Pit-1 whose infiltration rate of 0.25 cm/hr. Near to this test, ERT No. 5 was carried out using 24 electrode with 5 m electrode separation. The image exhibit a resistivity range of 15.3–49.2 Ωm with thickness of about 8 m indicating a saturated weathered formation (Fig. 7). The weathered formation was more on left and center portion of image, while on right side of the image, a resistivity of 158 Ωm was observed with thickness about 10–12 m indicating a semi-weathered formation followed by a high resistivity of $> 509 \Omega\text{m}$ indicating hard rock (Fig. 7). Similarly, infiltration test No. 4 carried

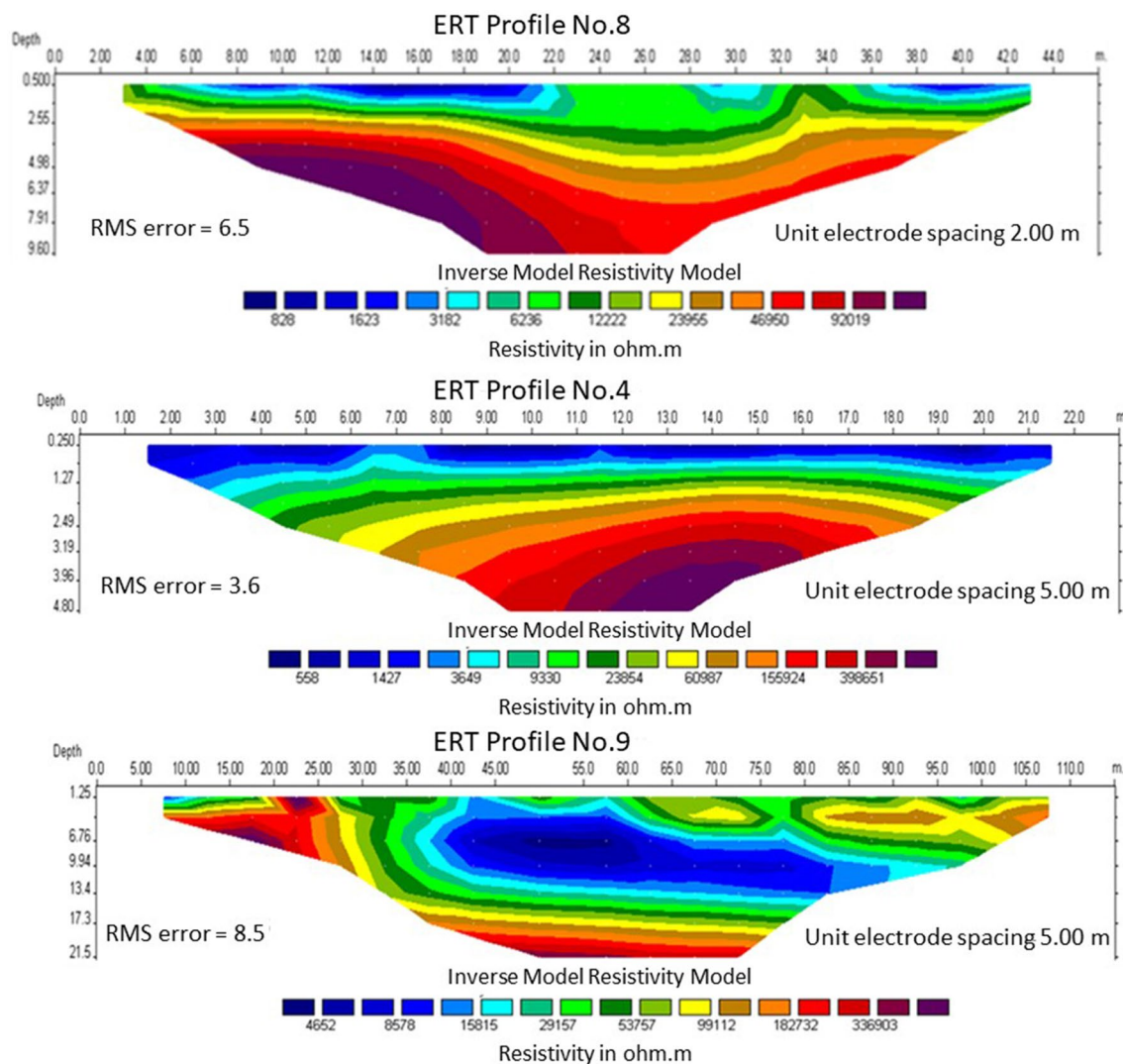


Fig. 6 ERT inverse model resistivity section of profile Nos. 8, 4 and 9 carried out inside and surrounding granite quarry Pit-1 near infiltration test No. 1

out in-between Pit-1 and Pit-2 having an infiltration rate of 0.09 cm/hr. Near this test, ERT No. 10 was carried out using 24 electrodes with 5 m electrode separation. ERT image

exhibit a resistivity range of 27.8–73.9 Ωm with very thin layer on left and center part of the image, while 3–4 m thickness on right side indicating saturated weathered formation,

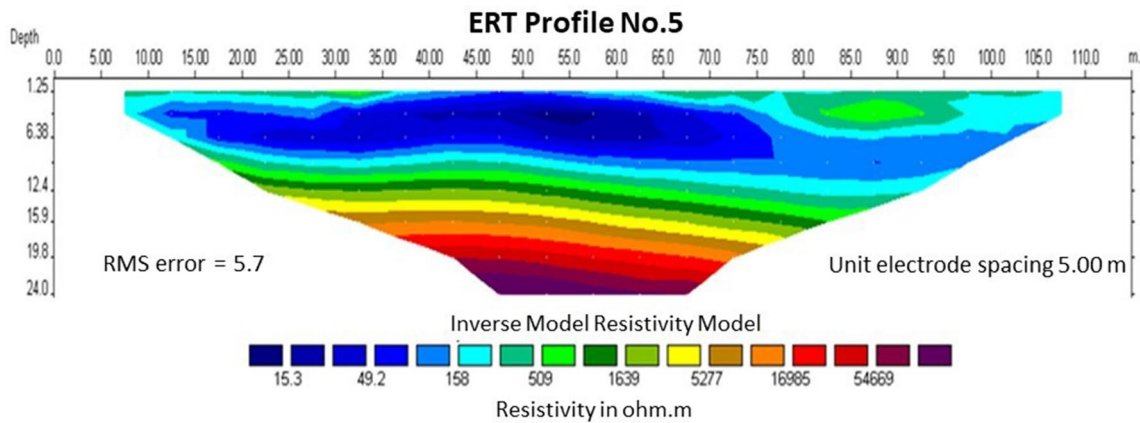


Fig. 7 ERT inverse model resistivity section of profile No. 5 carried out near Pit-1

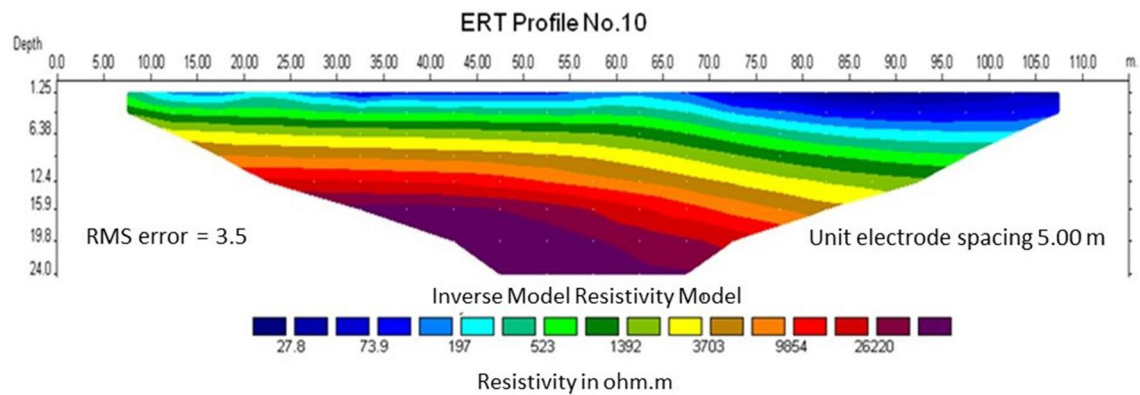


Fig. 8 ERT inverse model resistivity section of profile No. 10

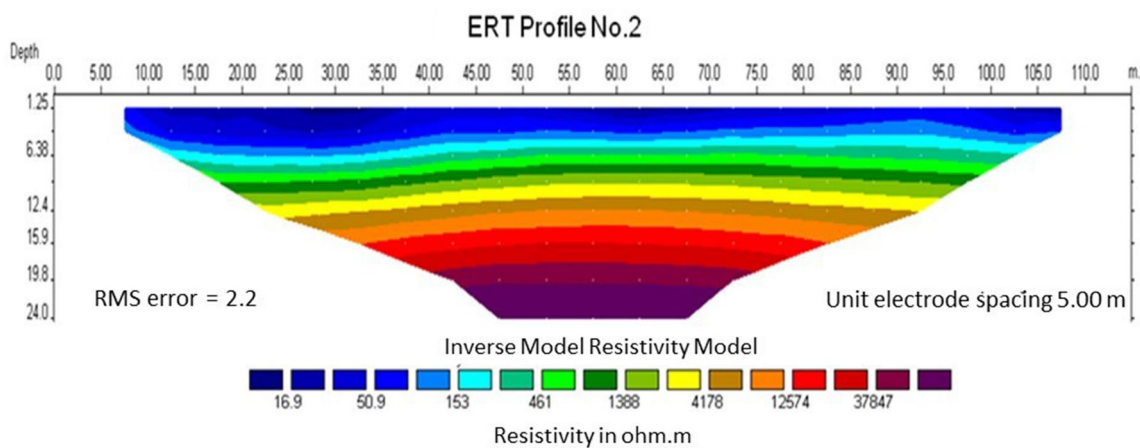


Fig. 9 ERT inverse model resistivity section of profile No. 2 carried out near Pit-2

followed by a thin layer of resistivity $197 \Omega\text{m}$ indicating a semi-weathered formation followed with high resistivity $> 523 \Omega\text{m}$ as a hard rock formation (Fig. 8). Infiltration test No. 5 carried out in southern side of Pit-2 having an infiltration rate of 10.2 cm/hr . Near this infiltration test, ERT No.2 was carried out using 24 electrodes with 5 m separation exhibiting resistivity ranges of $16.9\text{--}50.9 \Omega\text{m}$ with thickness of 2–6 m indicating saturated weathered formation. The weathered formation was more on left side compared to right and center part of image. Below this weathered formation, a thin layer of resistivity $153\text{--}461 \Omega\text{m}$ was observed indicating semi-weathered/fractured formation followed by high resistivity $> 1388 \Omega\text{m}$ indicating hard to very hard rock (Fig. 9).

Infiltration test No. 7 was conducted far away from Pit-1 in the eastern side having very low infiltration rate of 0.51 cm/hr . ERT profile 6 was laid near to this infiltration

test using 24 electrode with 5 m separation. ERT pseudo-section represents a resistivity range of $6.03\text{--}44.7 \Omega\text{m}$ with thickness of 5–10 m on right and left side exhibiting a highly saturated weathered formation, followed by an intermediate resistivity range of $122\text{--}332 \Omega\text{m}$ with thickness 8–10 m exhibiting weathered/semi-weathered formation. Below this, a high range of resistivity $> 903\text{--}6691 \Omega\text{m}$ was observed indicating hard rock formation (Fig. 10). Infiltration test No. 8 was north side of Pit-1 conducted near the tank having an infiltration rate 1.53 cm/hr . Near this test an ERT No. 11 was carried out using 24 electrodes with 5 m separation. ERT pseudo-section exhibit a low resistivity $11.2\text{--}21.7 \Omega\text{m}$ with thickness of about 6 m on left side and very thin thickness on right and center part of the image indicating highly saturated weathered portion due to the influence of the tank sub-surface moisture content. Another range of resistivity

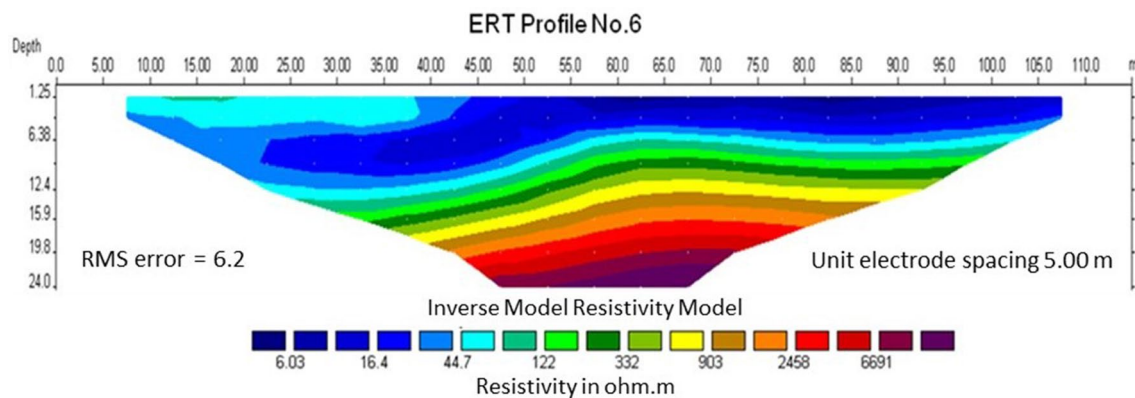


Fig. 10 ERT inverse model resistivity section of profile No. 6 carried out away from Pit-1

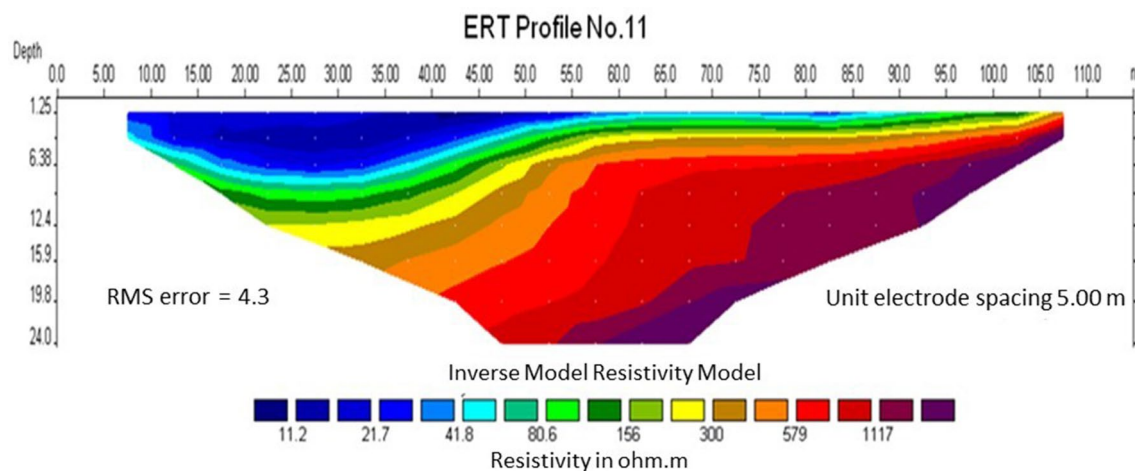


Fig. 11 ERT inverse model resistivity section of profile No. 11 carried out near tank

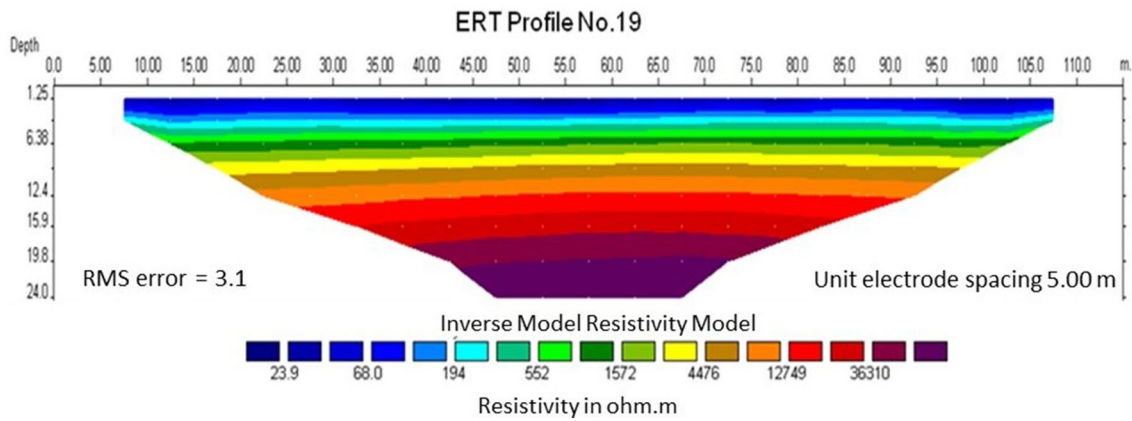


Fig. 12 ERT inverse model resistivity section of profile No. 19 carried out far away from Pit-1 and Pit-2

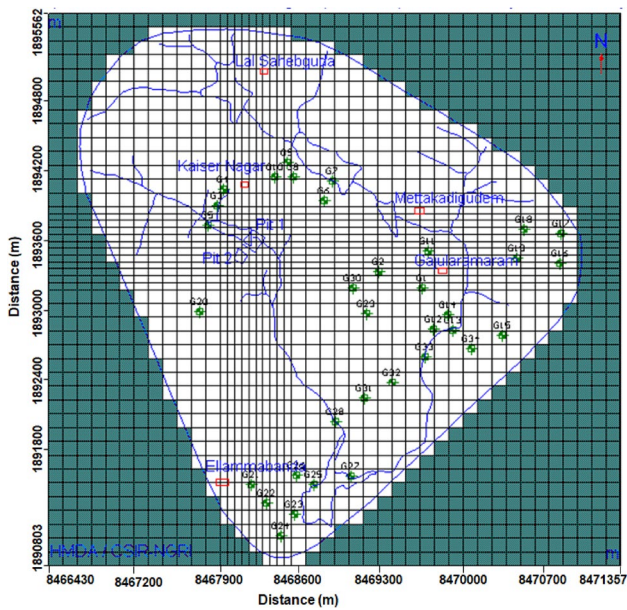


Fig. 13 Groundwater flow model domain in the study watershed

41.8–80.6 Ωm with very thin layer on right and center part of image compared to left side was observed indicating weathered formation, followed by a very thin layer of semi-weathered/fractured formation with resistivity of 156–300 Ωm was observed in the image, followed by high resistivity of $> 579 \Omega\text{m}$ indicating a hard rock formation (Fig. 11). Infiltration test No. 9 was conducted on southern side far away from the Pit-1 and Pit-2 having an infiltration rate of 10.2 cm/hr. Near this infiltration test, ERT No. 19 was conducted using 24 electrodes with 5 m electrode spacing. ERT pseudo-section represents a resistivity range of 22.9–68 Ωm with thickness of about 3 m indicating a highly

saturated weathered formation, followed by a resistivity of 194 Ωm with 2 m thickness indicating semi-weathered to fractured formation with high range of resistivity $> 552 \Omega\text{m}$ as hard to very hard rock formation (Fig. 12).

To assess the feasibility of seepages of hazardous effluents from quarry pits, a groundwater flow and mass transport model was conceptualized as a two-layer weathered and fractured aquifer system spread over an area of $4200 \times 4700 \text{ m}$ along with the observation wells considered for model calibration (Fig. 13). The permeability of saturated weathered and fractured zone was assumed as 1.0 m/day and was assigned in the model. Granite residual hills and ERT image resistivity data in the watershed prompted to reduce the permeability around the granite quarry pits. Accordingly, 0.1 m/day and 0.3 m/day were assigned to cells close to quarry pits and in the adjacent area, respectively (Fig. 14). The permeability has been assumed to be one-tenth of the horizontal permeability in the vertical direction. The simulated vertical cross-sections along Row 21 and Column 16 indicates that the weathered zone has a thickness of about 20 m and underlain fracture zone has 20 m thickness. The groundwater flow model has 46 rows and 45 columns of rectangular cells of varying sizes of $126 \times 116 \text{ m}$ (Fig. 13). Fine grid cells are used in and around the proposed quarry pit cells in the model. The watershed is spread over about 14.5 km^2 is a closed watershed with no flow boundary all along except the stream leaving from Ellammabanda tank as outlet. Constant head boundary condition was simulated in outflow region of the watershed with a groundwater head of 545 m (amsl). The streams joining the Ellammabanda tank have been simulated with a river boundary condition with appropriate stream stages and stream bed elevations. The intervening hydraulic conductance of stream bed and aquifer has been varying from 60 to $130 \text{ m}^2/\text{day}$ (Fig. 15). The Gajularamaram area receives rainfall of 850 mm mostly

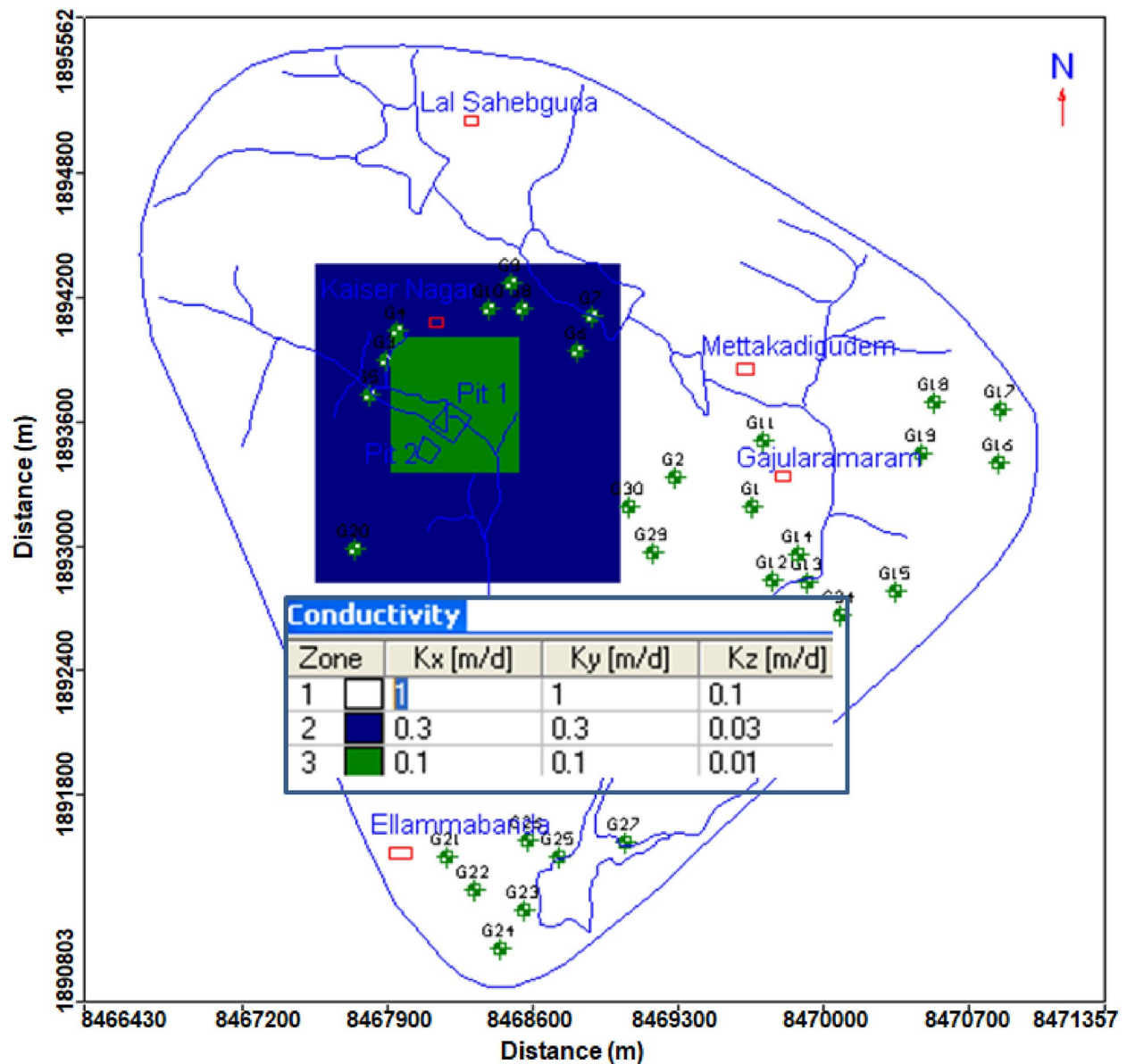


Fig. 14 Permeability distribution in the study watershed

during south-west monsoon period and natural groundwater recharge to the groundwater regime was poor due to local geological conditions. The groundwater recharge was assumed as 65 mm/year in the groundwater model for all over the watershed. Slightly lower groundwater recharge of 40 mm/year was assumed entering from the granite rocks surrounding the quarry pits (Fig. 16). The groundwater withdrawal from Kaiser Nagar and Lal Sahebguda habitations were reported poor yield. Accordingly, groundwater pumping was assigned to the wells in Kaiser Nagar and Gajularamaram villages varying from 20 to 40 m³/day. The

computed groundwater level contours in the groundwater flow model has been showing groundwater flow direction towards the stream joining the Ellammabanda tank and following closely the observed water level contours during July 2013 (Fig. 17a). The computed vs. observed hydraulic heads at 34 observation wells in the watershed have been found matching closely (Fig. 17b). The groundwater velocity field has been computed from the flow model using the hydraulic gradient and by assuming an effective porosity of 0.1. The computed groundwater velocity field represents an average groundwater velocity of < 10 m/year.

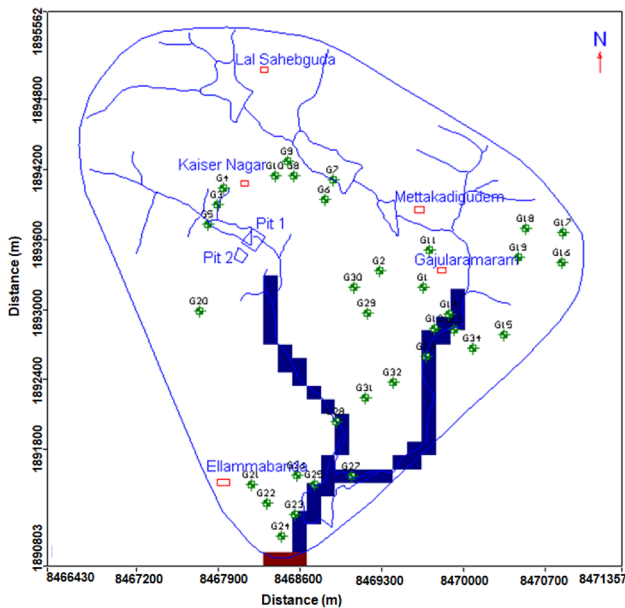


Fig. 15 Boundary conditions of groundwater flow model in the study watershed

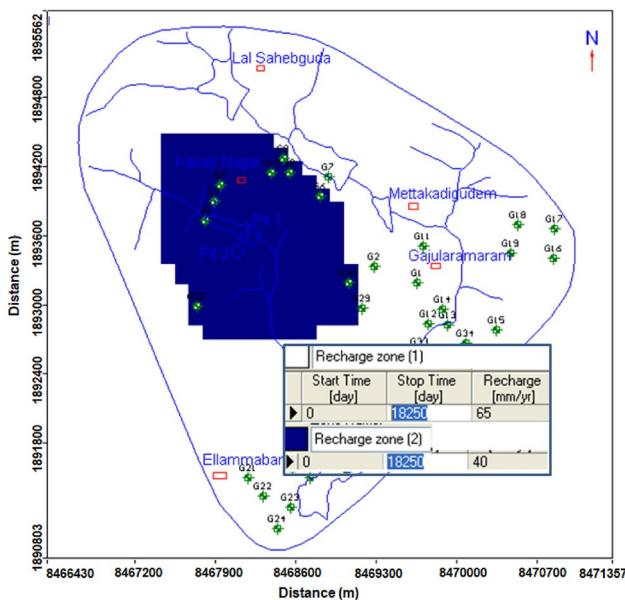


Fig. 16 Groundwater recharge to the groundwater flow model in the study watershed

Using the computed velocity field from the groundwater flow model, the mass transport model simulation was carried out using the MT3D software. The source concentration was assigned an average observed TDS concentration of 1500 mg/l around the granite quarry pits (Fig. 18). The initial concentration of groundwater was assumed as 600 mg/l. As regards dispersion parameters, longitudinal

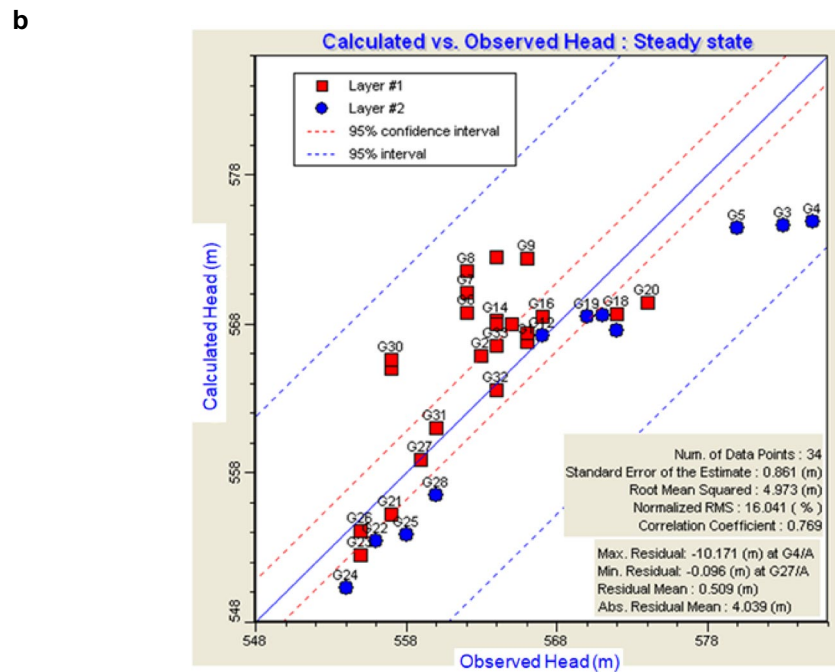
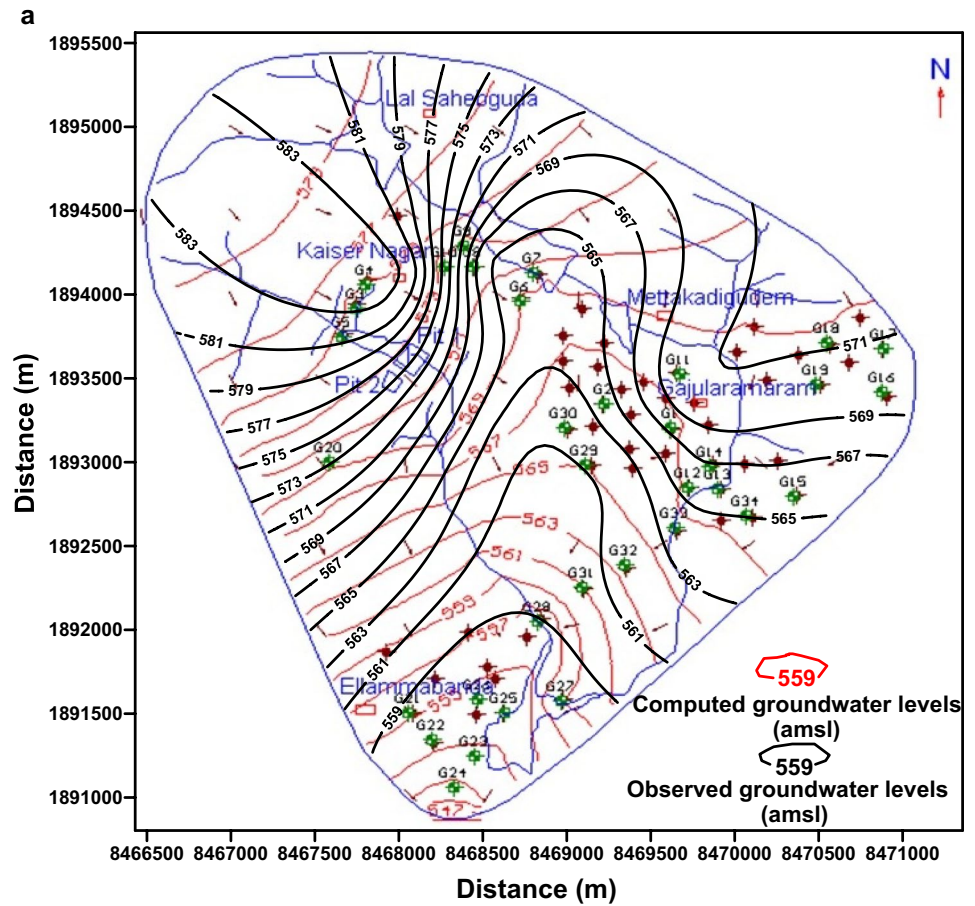
dispersivity was assumed as 10 m and horizontal to longitudinal and vertical to longitudinal dispersivity was also assumed as one-tenth and one-hundredth, respectively. The predicted TDS concentration plumes from both quarry pits in the mass transport model indicate that the migration of contaminant in groundwater is towards southeast direction of the pits. The predicted TDS concentration in groundwater for different years viz., 1, 10 and 50 years indicate that the TDS plume migration is limited to maximum distance of about 150 m from the Quarry pits in the south-eastern part (Figs. 19, 20 and 21). It is suggested to drill 5 observation wells for groundwater quality monitoring within 10 m from the proposed two quarry pits in the south and south-eastern parts for compliance monitoring of groundwater quality. The depth of wells should be about 50 m from ground surface.

The migration of TDS concentration plume along vertical direction was predicted for Column 16 for 5 and 50 years indicates that predicted TDS plume will be confined within the weathered zone adjacent to the quarry pits only during next 50 years (Fig. 22a, b). The vertical migration of TDS concentration from two quarry pits along Rows 19 and 20 for 50 years also indicate above inference of confinement of TDS plume within the weathered zone adjacent to the Quarry pits (Fig. 23a, b). The TDS plume migration has to be taken into consideration of the engineering the walls of the quarry pits wherever opening have been noticed during quarry operations before commissioning of the site for sediment filling with dredged sediments from Hussain Sagar Lake. The plume migration paths indicate limited area of likely groundwater contamination adjacent to the quarry pits in the downstream direction, which has to be protected from groundwater exploitation by public for the life cycle of the landfill.

Conclusions

Groundwater level monitoring was carried out in 34 observation wells in the watershed covering Gajularamaram area indicated that there exists a steep hydraulic gradient with regard to the groundwater movement around the proposed granite quarry pits; the groundwater flow direction is from north-west to the southeast. The depth to groundwater levels and withdrawals show that groundwater potential is poor in the immediate vicinity of quarry pits particularly in the villages of Kaiser Nagar and Lal Sahebguda in the upstream. This groundwater condition revealed that lateral groundwater movement is very slow and there is very little possibility of groundwater entering from upstream area through hard granite rocks into the quarry pits. The low infiltration rate near quarry pits also suggested that negligible possibility of recharge due to rainfall. Electrical Resistivity Tomography survey inside the quarry pits as well as in the surrounding

Fig. 17 **a** Computed and observed groundwater contours of groundwater flow model in the study watershed. **b** Computed vs. observed groundwater level in the groundwater flow model of study watershed



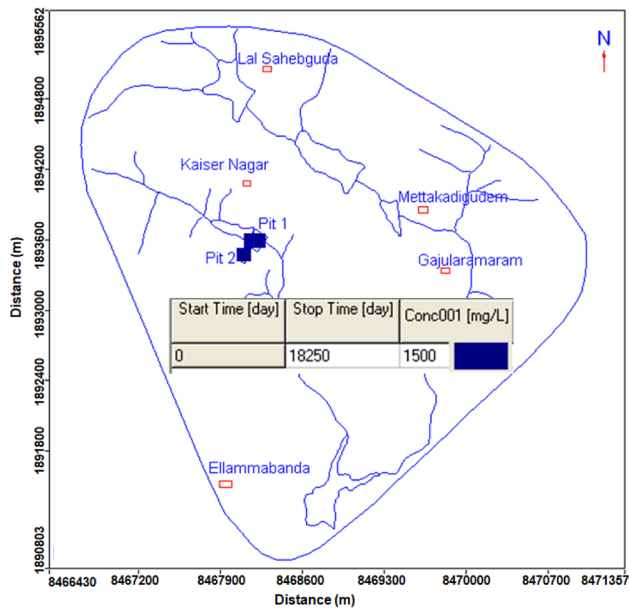


Fig. 18 Expected leachate loading of TDS (mg/l) in the granite quarry pits in the mass transport model

area projected extension of high resistivity granite rocks from quarry pits towards south and eastern parts. This hard rock will impede groundwater movement from quarry pits towards the downstream. The groundwater flow and mass transport modeling in the watershed has quantified likely TDS plume migration confining to maximum of 150 m from the quarry pit boundary towards south and southeast during next 50 years. The vertical migration of the TDS plume will be restricted to the weathered zone adjacent to the quarry Pit-1 and Pit-2 only. Based on the electrical resistivity characteristics inferred from the ERT imaging, hydrogeological investigations, in situ infiltration measurements and mass transport modeling study for likely contaminant migration from the quarry pits, it is recommended that the proposed granite quarry Pit-1 and Pit-2 in Gajularamaram village is a suitable site for disposal of dredged hazardous sediments from Hussain Sagar Lake. Little engineering on side walls of the pits have to be undertaken to close the opened joints and fissures occurred during blasting of the quarry for granite excavation for arresting lateral migration of leachate if any, through them. Recommended, drilling of five observation wells up to 50 m depth within 10 m radius from the quarry pits in south and south-eastern parts of the downstream side.

Fig. 19 TDS plume concentration from mass transport model in the study watershed—after 1 year

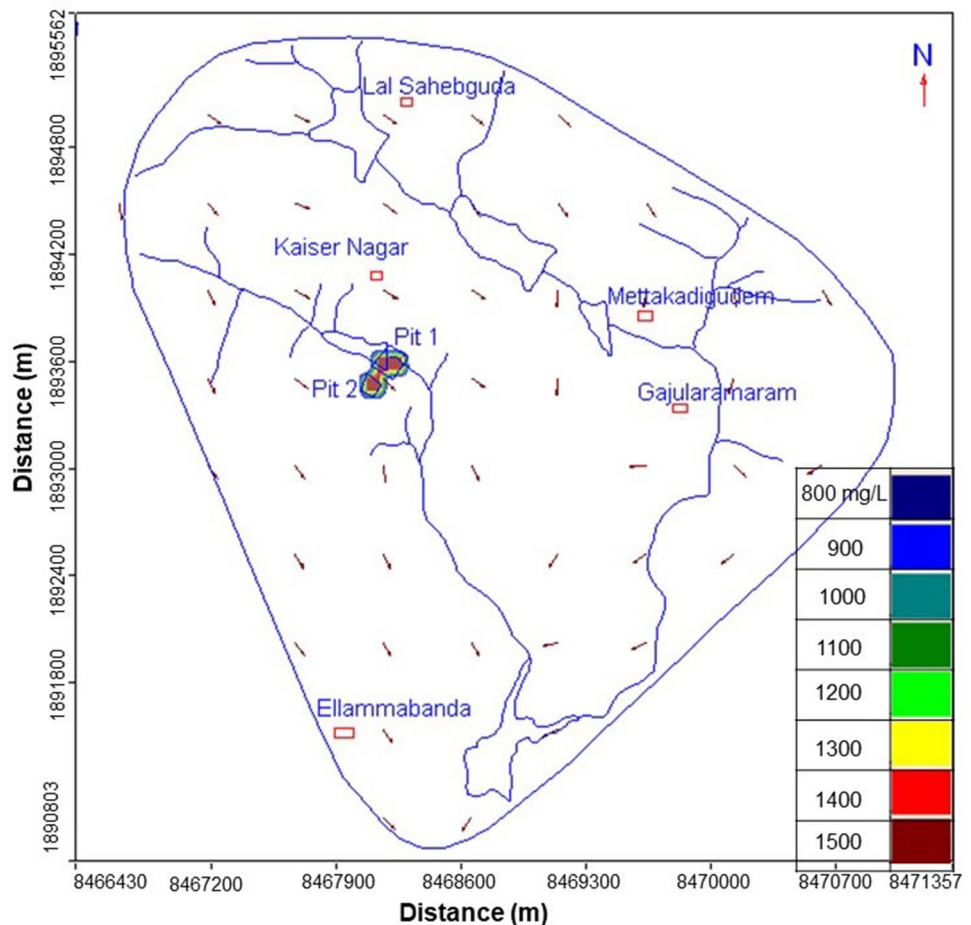
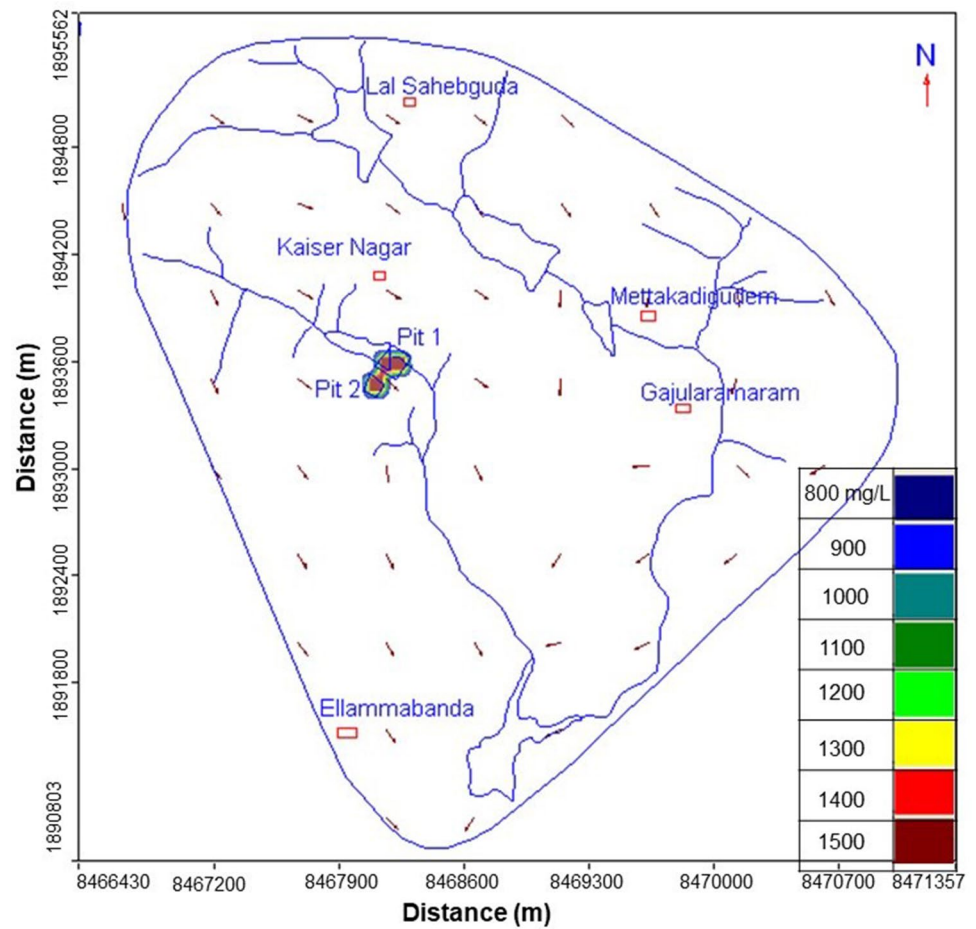


Fig. 20 TDS plume concentration from mass transport model in the study watershed—after 10 years



Flooding of storm water runoff in the quarry pits avoided during monsoon. Periodical monitoring of groundwater quality is also suggested in these monitoring wells for

ascertaining and assessing functioning of the land fill in the quarry and also for compliance monitoring as per State Pollution Control Board norms.

Fig. 21 TDS plume concentration from mass transport model in the study watershed covering—after 50 years

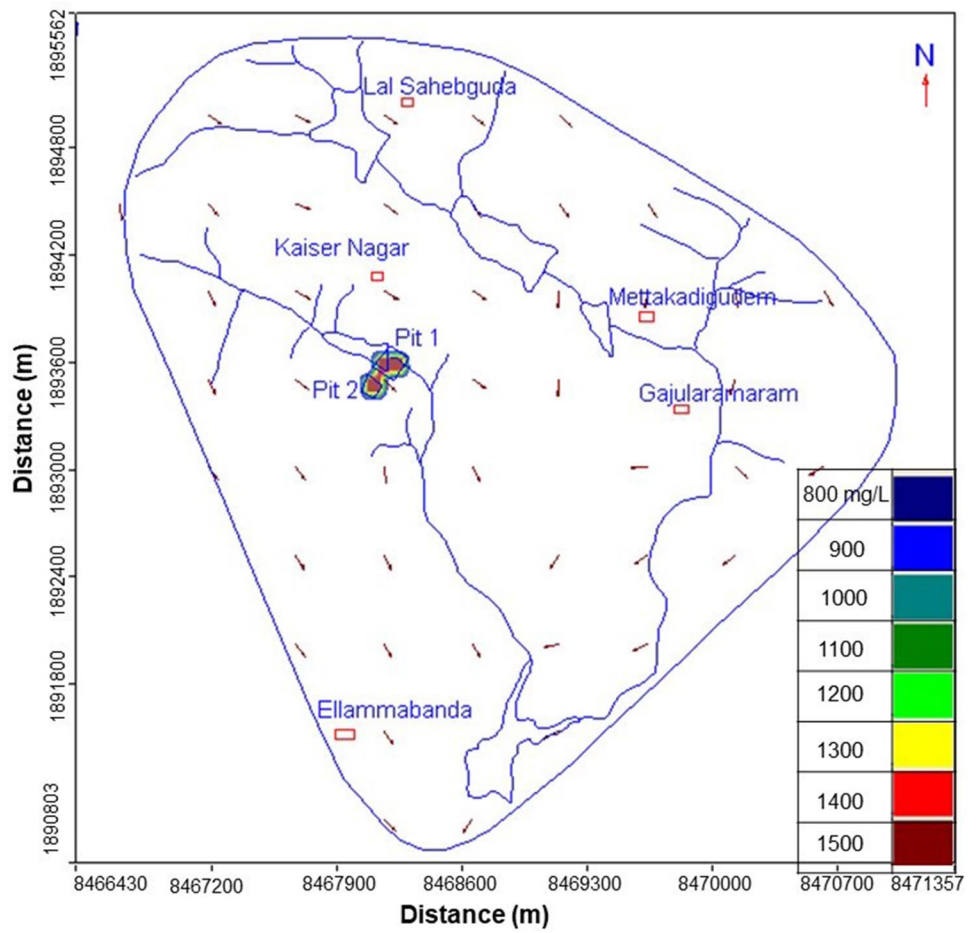


Fig. 22 a, b TDS vertical plume concentration from mass transport model in the study watershed—after 5 and 50 years in column 16

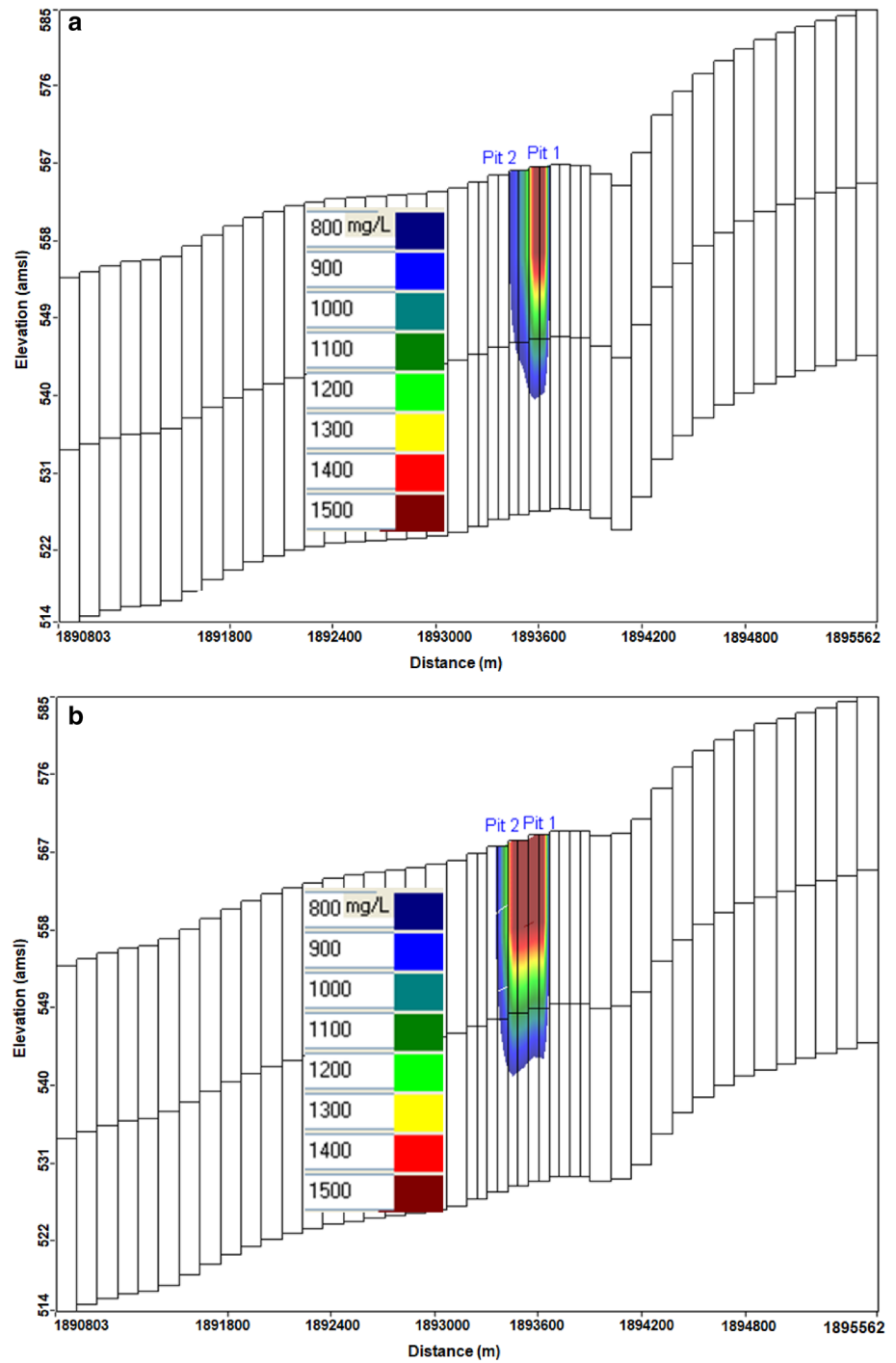
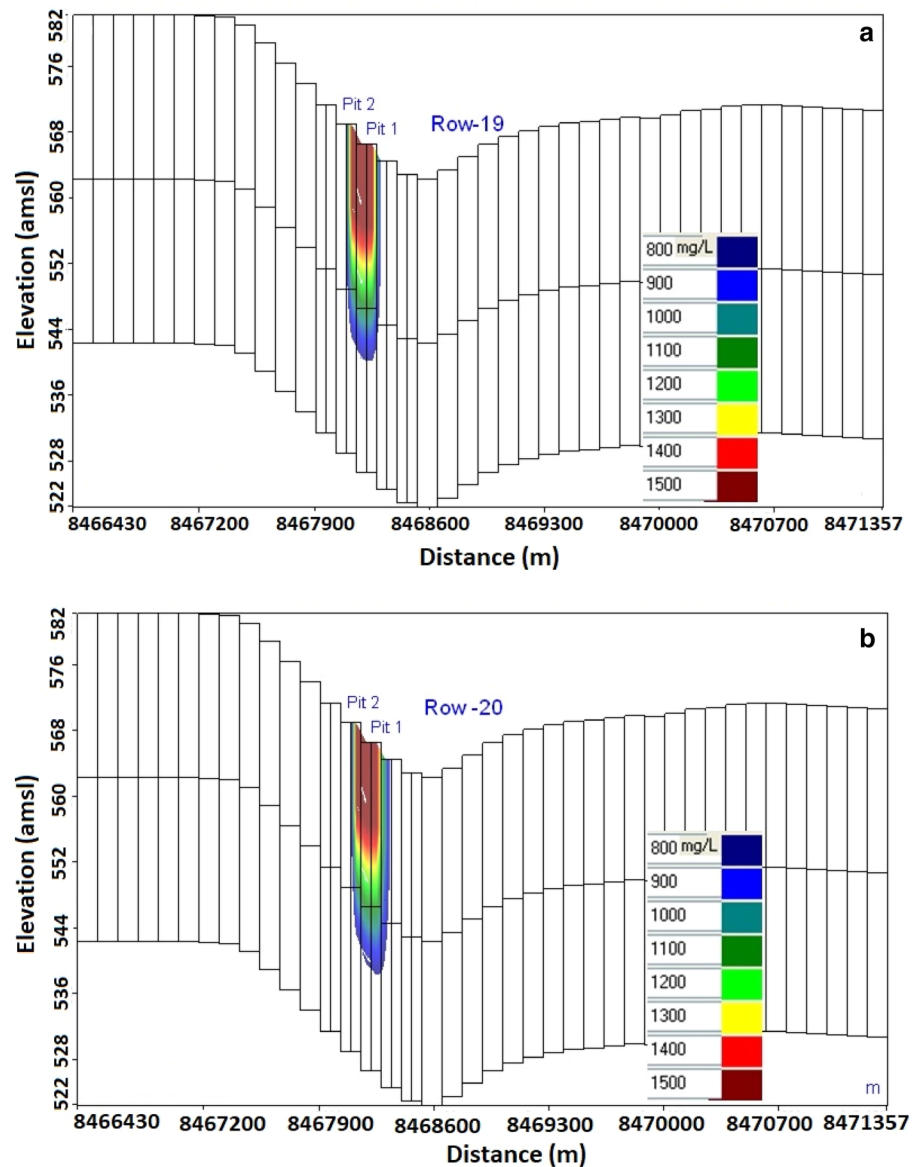


Fig. 23 a, b TDS vertical plume concentration from mass transport model in the study watershed—after 50 years in row 19 and row 20



Acknowledgements The authors are thankful to the Director, NGRI, Hyderabad, for his encouragement to publish this paper. The authors also express their sincere thanks to the HMDA for sponsoring the project to the NGRI. Authors express their sincere thanks to the Editor-in-Chief and Guest Editor for their encouragement and support. Authors also thanks to the reviewers for their constructive and scientific suggestion for improving the manuscript standard. The manuscript Reference No. is NGRI/Lib/2020/Pub-72.

Declarations

Conflict of interest No conflict of interest to declare.

References

- Abushammala MFM, Basri NEA, Basri H, Kadhum AAH, El-Shafie AH (2010) Estimation of methane emission from landfills in Malaysia using the IPCC 2006 FOD model. *J Appl Sci* 10:1603–1609
- Allen AR, Dillon AM, O'Brien M (1997) Approaches to landfill site selection in Ireland. In: Marinos PG, Koukis GC, Tsiambaos GC, Stournaras GC (eds) *Engineering geology and the environment*. Balkema, Rotterdam, pp 1569–1574
- Alslaibi TM, Mogheir YK, Afifi S (2011) Assessment of groundwater quality due to municipal solid waste landfills leachate. *J Environ Sci Technol* 4:419–436
- Aristodemou E, Thomas-Betts A (2000) DC resistivity and induced polarization investigations at a waste disposal site and its environments. *J Appl Geophys* 44:275–302
- Atekwana EA, Sauck WA, Werkema Jr DD (2000) Investigations of geoelectrical signatures at a hydrocarbon contaminated site. *J Appl Geophys* 44(2–3):167–180
- Bagchi A (1994) *Design, construction and monitoring of landfills*, 2nd edn. Wiley, New York, pp 7–19
- Bear J (1979) *Hydraulics of groundwater*. McGraw-Hill, New York, p 241
- Beres M, Haeni FP (1991) Application of ground penetrating radar methods in hydrogeologic studies. *Ground Water* 29(3):375–386

- Bernstone C, Dahlin T, Ohlsson T, Hogland W (2000) DC-resistivity mapping of internal landfill structures: two pre excavation surveys. *Environ Geol* 39(3–4):360–370
- Bhukosh (GSI) <http://bhukosh.gsi.gov.in/Bhukosh/Public>
- Davis JL, Annan AP (1989) Ground penetrating radar for high resolution mapping of soil and rock stratigraphy. *Geophys Prospect* 37:531–551
- Dawson CB, Lane JW Jr, White EA, Belaval M (2002) Integrated geophysical characterization of the Winthrop landfill southern flow path, Winthrop, Maine. In: Proceedings of the symposium on the application of geophysics to engineering and environmental problems. Environmental and Engineering Geophysical Society, Denver. Las Vegas, Nevada, p 22
- DELG (Department of Environment and Local Government) (1998) A policy statement, waste management changing our ways. ENFO-Information on the Environment (http://www.enfo.ie/pub_main.htm#wm)
- DELG (Department of Environment and Local Government) (1999) Environment protection agency and geological survey of Ireland. Groundwater protection schemes, p 24
- Domenico PA, Schwartz FW (1990) Physical and chemical hydrogeology. Wiley, New York, p 824
- EPA (Environmental Protection Agency) (1995) Landfill manuals. Investigations for landfills. EPA, Wexford
- EPA (Environmental Protection Agency) (1996) Landfill manuals. Manual on site selection (2nd draft). EPA, Wexford
- EPA (Environmental Protection Agency) (1997) Landfill manuals. Landfill operational practices. EPA, Wexford
- EPA (Environmental Protection Agency) (1999a) Landfill manuals. Landfill restoration and after care. EPA, Wexford
- EPA (Environmental Protection Agency) (1999b) Proposed national hazardous waste management plan. EPA, Wexford
- Georgaki I, Soupios P, Sakkas N, Ververidis F, Trantas E, Vallianatos F, Manios T (2008) Evaluating the use of electrical resistivity imaging technique for improving CH₄ and CO₂ emission rate estimations in landfills. *Sci Total Environ* 389(2–3):522–531
- Green A, Lenz E, Maurer H (1999) A template for geophysical investigations of small landfills. *Leading Edge* 18(2):248–254
- Guiger N, Franz T (1996) Visual MODFLOW: users guide. Waterloo Hydrogeologic (WHI), Ontario
- Heitfeld KH, Heitfeld M (1997) Siting and planning of waste disposal facilities in difficult hydrogeological conditions. In: Marinou K, Tsiambaos S (eds) Engineering geology and the environment. Balkema, Rotterdam, pp 1623–1628
- Hillary GT, Samuel V (1993) Integrated solid waste management engineering principles and management issues. McGraw-Hill International Editions, New York
- Jain CK, Gurunadha Rao VVS, Prakash BA, Mahesh Kumar K, Yoshida M (2010) Metal fractionation study on bed sediments of Hussainsagar lake, Hyderabad, India. *Environ Monit Assess* 166:57–67
- Jorge LP, Walter MF, Vagner RE, Fisseha S, Joao CD, Helyelson PM, (2004) The use of GPR and VES in delineating a contamination plume in a landfill site: a case study in SE Brazil. *J Appl Geophys* 55(3–4):199–209
- Karlik G, Kaya MA (2001) Investigation of groundwater contamination using electric and electromagnetic methods at an open waste-disposal site: a case study from Isparta. *Turkey Environ Geol* 40(6):725–731
- Kenny B (1995) Chemical pollution: Gujarat's toxic corridor. The Hindu survey of the environment 95. Kasturi & Sons Ltd., Chennai, pp 163–166
- Konikow LF, Grove DB (1977) Derivation of equations describing solute transport in groundwater, water resources investigations. *US Geol Surv* 77:19–30
- Langer M (1995) Engineering geology and waste disposal: scientific report and recommendations of the IAEG commission No. 14. *Bull Intl Assoc Eng Geol* 51:29
- Lanz E, Jemmi L, Muller R, Green A, Pugin A, Huggenberger P (1994) Integrated studies of Swiss waste disposal sites: results from geo radar and other geophysical surveys. In: Proceedings of the 5th international conference on ground penetrating radar (GPR 94). Kitchener, Ontario, p 1261–1274
- Li-Wen CAO, Yun-Huan C, Jing Z, Xiao-Zhi Z, Cui-Xia L (2006) Application of grey situation decision making theory in site selection of a waste sanitary landfill. *J China Univ Min Technol* 16(4):393–398
- Loke MH, Barker RD (1996) Rapid least-squares inversion of apparent resistivity pseudo sections by a quasi-Newton method. *Geophys Prospect* 44:131–215
- Mather JD (1995) Preventing groundwater pollution from landfilled waste—is engineered containment an acceptable solution. In: Nash H, McCall GJH (eds) Groundwater quality. Chapman & Hall, London, pp 191–195
- Mirbagheri SA, Esfeh KHR (2008) Finite element modelling of leaching from a municipal landfill. *J Appl Sci* 8:629–635
- Nair M (1999) Industrial pollution: belligerent attitude. The Hindu survey of the environment 99. Kasturi & Sons Ltd., Chennai, pp 179–183
- Orlando L, Marchesi E (2001) Geo radar as a tool to identify and characterise solid waste dump deposits. *J Appl Geophys* 48:163–174
- Prafal B (1996) Toxic waste disposal: a ready dumping lot. The Hindu survey of the environment 96. Kasturi & Sons Ltd., Chennai, pp 185–191
- Saltas V, Vallianatos F, Soupios P, Makris JP, Triantis D (2005) Application of dielectric spectroscopy to the detection of contamination in sandstone. In: international workshop in geoenvironment and geotechnics, September 2005, Milos Island, Greece, p 269–274
- Sauck WA (2000) A model for the resistivity structure of LNAPL plumes and their environs in sandy sediments. *J Appl Geophys* 44:151–165
- Sauck WA, Atekwana EA, Nash MS (1998) Elevated conductivities associated with an LNAPL plume imaged by integrated geophysical techniques. *J Env Eng Geophys* 2(3):203–212
- Soupios P, Manios T, Sarris A, Vallianatos F, Maniadakis K, Papadopoulos N, Makris JP, Kouli M, Gidarakas E, Saltas V, Kourgialas N (2005a) Integrated environmental investigation of a municipal landfill using modern techniques. In: international workshop in geo environment and geotechnics, Milos Island, Greece, p 75–82
- Soupios P, Vallianatos F, Papadopoulos I, Makris JP, Marinakis M (2005b) Surface- geophysical investigation of a landfill in Chania, Crete. In: international workshop in geo environment and geotechnics, Milos Island, Greece, p 149–156
- Soupios P, Vallianatos F, Makris JP, Papadopoulos I (2005c) Determination of a landfill structure using HVSR, geoelectrical and seismic tomographies. In: international workshop in geo environment and geotechnics, Milos Island, Greece, p 83–90
- Srikanth R, Madhumohan Rao A, Shravan Kumar Ch, Anees K (1993) Lead, cadmium, nickel and zinc contamination of groundwater around Hussain Sagar lake. *Bull Environ Contam Toxicol* 50:138–143
- Stanton GP, Schrader TP (2001) Surface geophysical investigation of a chemical waste landfill in Northwestern Arkansas. In: EL Kuniandy (ed) Presented in 2001 U.S. geological survey karst interest group proceedings. Water resources investigations report 01–4011, p 107–115
- Sunny S (1997) Bichri's saga: a triumph of collective will. The Hindu survey of the environment 97. Kasturi & Sons Ltd., Chennai, pp 183–187
- Wentz-Charles A (1995) Hazardous waste management, McGraw Hill international editions, chemical engineering series, 2nd edn. McGraw Hill Inc, Singapore, pp 80–86 (296–351)

Publisher's Note Springer Nature remains neutral with regard to jurisdictional claims in published maps and institutional affiliations.